Reaction cross sections and rate constants for the F+H₂(D₂)→HF(DF)+H(D) reactions from quasiclassical trajectory calculations on a potential energy surface

Reaction cross sections and rate constants for the $F+H_2(D_2)\rightarrow HF(DF)+H(D)$ reactions from quasiclassical trajectory calculations on a potential energy surface

F.J. Aoiz [a], L. Bañares [a], V.J. Herrero [b], K. Stark [c], H.-J. Werner [c]

[a] *Departamento de Química Física, Facultad de Química, Universidad Complutense, 28040 Madrid, Spain*
[b] *Instituto de Estructura de la Materia (CSIC), Serrano 123, 28006 Madrid, Spain*
[c] *Institut für Theoretische Chemie, Universität Stuttgart, Pfaffenwaldring 55, D-70569 Stuttgart, Germany*

Abstract

The dependence of the cross sections for the $F+H_2$ and $F+D_2$ reactions on the collision energy has been determined by means of quasiclassical trajectory calculations (QCT) on the Stark and Werner (SW) ab initio potential energy surface (PES). From these data rate constants as a function of temperature have been evaluated. For both reactions, fairly good agreement between the calculated and experimental rate constants is obtained. Our results are compared with previous QCT and quantum mechanical (QM) calculations on other PES, as well as with recent approximate QM results on the SW-PES. The rate constants are in close agreement for the $F+D_2$ reaction, while for $F+H_2$ our values are larger than the ones obtained on the 6SEC-PES. The more orienting character of the SW-PES can explain these differences, when the nuclear spin statistics of H_2 and D_2 are taken into account.

1. Introduction

The $F+H_2$ system has been a prototype in reaction dynamics for decades, especially since the memorable cross beam experiments of Lee and co-workers [1,2]. Recently, interest in this reaction has been renewed, mainly due to the appearence of higher resolution measurements [3-7] and new potential energy surfaces (PES) [8-13]. The accuracy of these new PES has been tested extensively by comparing the results of dynamical calculations [3,4,9,14-26] to the growing set of experimental data.

To date, the best global agreement between experiment and theory was obtained with the ab initio PES of Stark and Werner [12,13] (hereafter SW). Qua-

siclassical trajectory (QCT) calculations [20-22] as well as full quantum mechanical (QM) calculations [25] performed on this surface could quite satisfactorily reproduce most of the experimental data on product state distributions and differential cross sections. Quantum mechanical calculations allowed the simulation and interpretation of the FH_2^- electron photodetachment spectra of Neumark and co-workers [3]. The QCT and QM differential cross section mainly differed in the amount of the state-specific forward scattering; the forward peaks were underestimated in the QCT calculations, due to significant tunneling effects at large impact parameters [25]. On the other hand, the forward peaks obtained in the QM calculations were larger than those observed experimentally [1,2],

indicating that the combined classical and centrifugal barrier on the SW surface is somewhat too low. In fact, the effect of spin–orbit coupling in the entrance channel, which has not been taken into account in the PES so far, will increase the barrier height by about 20% [13].

While the differential cross sections and relative product distributions are sensitive to the shape of the potential energy surface, the absolute values of the cross sections and the reactive rate constants are expected to depend crucially on the absolute height of the reaction barrier. This is clearly examplified in the case of the empirical PES developed by Takayanagi and Sato [9] (herafter TS), which performs quite well for the detailed dynamical observables [9,19], but yields reaction rate constants that are significantly larger than the experimental ones [19]. It is therefore of interest to compute the rate constants using the new SW-PES, which has a significantly higher barrier than the TS-PES. In fact, recent calculations using the coupled states approximation are in general good agreement with the measurements [26]

In this Letter we report the results of quasiclassical trajectory calculations of rotational state selective absolute cross sections, rate constants, as well as thermal rate constants in the range of temperatures between 200 and 500 K. The calculations have been carried out for the F+H$_2$ and F+D$_2$ isotopic variants using the SW potential energy surface. The results are discussed and compared with experimental data and previous calculations.

2. Method

The general method for the calculation of quasiclassical trajectories has been described previously (see Refs. [27,28] and references cited therein). The rate constants for selected rotational states of the reactants are obtained from the corresponding excitation functions, i.e. the collision energy (E_T) dependence of the reaction cross section, $\sigma_R(E_T)$. The usual way to calculate excitation functions in QCT calculations consists of computing batches of trajectories, each of them at a given collision energy and at an internal quantum state of the reactive diatom. In order to improve the computational efficiency, however, the collision energies of the trajectories were sampled randomly within

the interval [E_1, E_2] for each of the relevant rotational states of H$_2$ and D$_2$. The lower limit E_1 of the energy interval was chosen below the threshold for reaction, and the upper limit was 0.8 eV. Once a collision energy had been chosen within this given interval, the impact parameters were obtained by sampling randomly between zero and a maximum value, b_{max}, calculated from the line-of-the-centers expression [28]

$$b_{max}(E_T) = D\left(1 - \frac{E_D}{E_T}\right)^{1/2}, \qquad (1)$$

where D and E_D were obtained by fitting the values of the maximum impact parameters found by running a small number of trajectories at several selected collision energies to the expression of Eq. (1). The parameters E_D and D were chosen such that no reactive trajectories occur for even somewhat smaller impact parameters than those given by Eq. (1) (see Ref. [28] for more details).

For the temperature range of the present study, rotational numbers up to $j = 5$ had to be included for H$_2$ and up to $j = 6$ for D$_2$. All the calculations were performed for the ground vibrational state of the molecules. A batch of 60000 trajectories was run for each rotational state. The tests of energy and of angular momentum conservation, the selection of initial states and the assignment of final states were done as described earlier [27].

In previous studies the quantization was made by equating the square of the rotational H$_2$ and D$_2$ angular momentum to $j(j + 1)\hbar^2$, where j is the corresponding quantum number. However, Azriel et al. [29] recently pointed out that the use of the semiclassical quantization $(j + 1/2)^2\hbar^2$, known as the Langer correction, produces a better agreement with exact QM calculations. The addition of a 'residual' rotation for $j = 0$ also improves the agreement with experimental results, especially in the case of the SW-PES. We have thus adopted this quantization scheme, which produces (slightly) different results to the $j(j + 1)$ quantization only for $j = 0$.

3. Results and discussion

The excitation functions for the F+H$_2$ and F+D$_2$ reactions calculated on the SW-PES between threshold and 0.7 eV are shown in Fig. 1. In all cases, the reac-

$F+H_2(v=0,j) \rightarrow HF+H$

S-W PES

j=0
j=1
j=2
j=3
j=4
j=5

$F+D_2(v=0,j) \rightarrow DF+D$
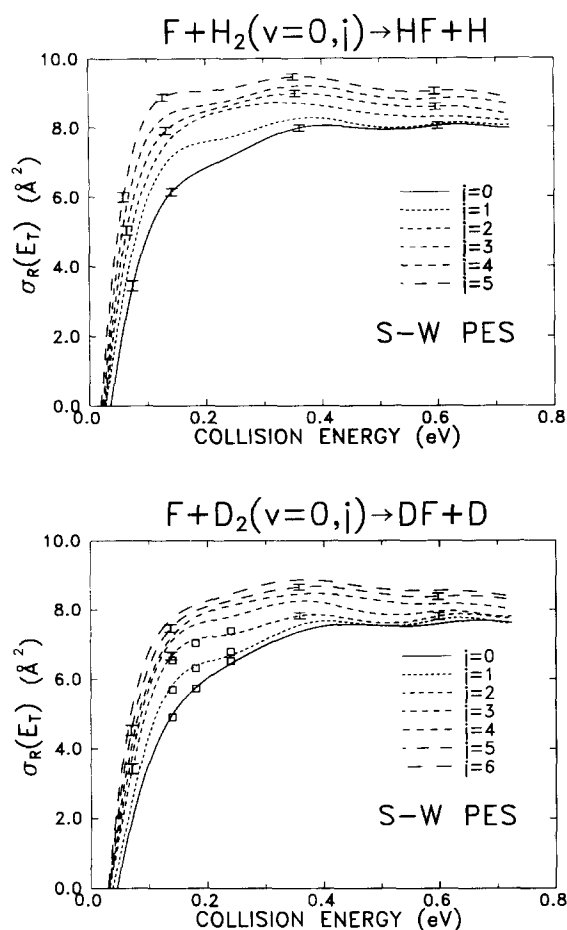
S-W PES

j=0
j=1
j=2
j=3
j=4
j=5
j=6

Fig. 1. Total reaction cross section as a function of collision energy (excitation function) calculated by QCT on the SW-PES for the reaction of fluorine atoms with hydrogen (deuterium) molecules in selected rotational states of the ground vibrational state. Upper panel: F+H_2; lower panel: F+D_2. The error bars represent one standard deviation of the calculation. The squares in the lower panel correspond to QCT calculations carried out at a single collision energy (60000 trajectories each), and are shown to illustrate the accuracy of the method used for calculating the excitation functions.

tion cross section increases abruptly after the threshold and reaches a constant value at $E_T = 0.2$–0.4 eV. Increasing the rotational excitation of the H_2 and D_2 molecules results in a diminution of the threshold energy and in a sharper rise in the post-threshold cross sections. An enhancement of the reactivity with the rotational excitation of H_2 was also obtained in dynamical calculations [19,23] on the 6SEC-PES of Truhlar and co-workers [11] and most notably on the TS-

PES [19]. In the latter case, the effect was so extreme that the reaction was found to have no threshold for H_2 molecules in rotational states other than $j = 0$. As a result of that, the corresponding room temperature rate constants calculated on the TS-PES were much larger than the experimental ones, as already mentioned. The present results are rather similar to those obtained on the 6SEC surface [23], but the beneficial effect of rotation on reactivity is more pronounced on the more orienting SW-PES. This is shown in Fig. 2, where the QCT cross sections are compared for the two isotopic variants of the reaction on the two potential energy surfaces. The threshold for the $F+H_2$ reaction on the SW-PES is always smaller than that obtained on the 6SEC-PES irrespective of the initial j. Therefore, despite the fact that the SW-PES barrier height is slightly larger than that of 6SEC-PES, especially for the perpendicular approach, the more orienting character of the surface causes the SW-PES to be more reactive than the 6SEC one. Furthermore, whereas on the 6SEC-PES the threshold energy does not seem to change with j, on the SW-PES the threshold for $j = 0$ is clearly higher than that for $j > 0$. In the case of the SW-PES, the reaction cross section at a given collison energy increases monotonically with growing j, for all the j values investigated, whereas the $\sigma_R(E_T, j)$ on the 6SEC-PES are similar for $j > 2$. The insert of Fig. 2 also shows the Boltzmann distribution of collision energies at $T = 300$ K. Since the $\sigma_R(E_T)$ obtained on the SW-PES is larger than that on the 6SEC in this region near the threshold, one can expect a larger rate constant.

In the reaction of fluorine atoms with the heavier deuterium molecules, there is also a shift of the threshold towards lower collision energies with increasing j, reflecting the orienting effects of the SW surface (see Fig. 2). In this case, only for $j > 2$ the threshold energies for reaction on this PES are lower than those on the 6SEC surface (which are independent of the rotational quantum number).

QM calculations [24] of excitation functions using the coupled states approximation for both isotopic variants on the 6SEC-PES were shown to be in excellent agreement with the QCT ones [23], the only noticeable discrepancy being the $F+H_2(j = 0)$ reaction, where QM cross sections are higher than those from QCT. In particular, the quantal and classical thresholds are almost the same for all the initial rotational
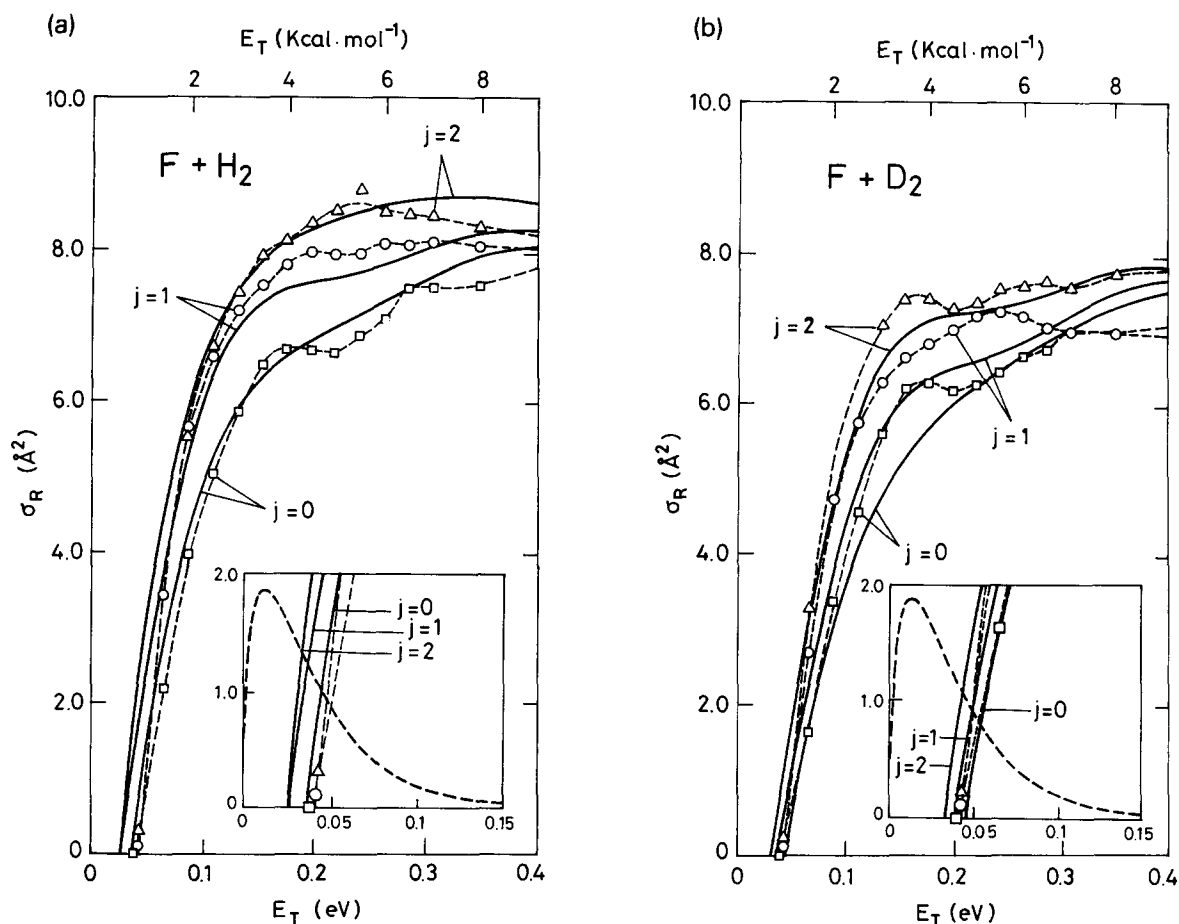
Fig. 2. Comparison of the QCT total reaction cross sections as a function of the collision energy, E_T, calculated on the 6SEC-PES, taken from Ref. [23] (dashed line with squares for $j = 0$, circles for $j = 1$, and triangles for $j = 2$), and on the SW-PES (solid line) calculated in the present work. (a) F+H$_2$; (b) F+D$_2$. The inserts show the threshold region and the Boltzmann E_T distribution at 300 K (dashed line).

states considered. In contrast to that, the present classical excitation functions on the SW-PES have higher thresholds than those from the recent coupled states calculations [26] on the same PES, which are practically zero in all cases.

The excitation functions shown in Fig. 1 were used to calculate thermal rate constants $k(T; j)$ for each of the initial rotational states. The values obtained are listed in Table 1 and do not include the 'multisurface correction factor' (see below). As expected, the enhancement of reactivity due to rotational excitation is more marked at low temperatures. At $T = 200$ K, the rate constant for F+H$_2$($j = 0$) is more than three times smaller than that for $j = 5$, but at $T = 500$ K the difference of these rate constants is less than a factor

of two. The same trend is also found in the reaction of F+D$_2$.

Thermal rate constants $k(T)$ for both reactions were obtained between 200 and 500 K from the $k(T; j)$ after the appropriate weighting with the distribution of rotational states of the molecules. The results are listed in Table 2 and represented in Fig. 3, where they are compared to the experimental data [30–32] and to the QCT rate constants of Rosenman and Persky on the 6SEC-PES [23]. In order to make the results directly comparable to experiment in this case the 'multisurface correction factor' is included (see for instance Ref. [18] and references cited therein), which accounts for the statistical population of the asymptotic $^2P_{3/2}$ and $^2P_{1/2}$ states, assuming that non-adiabatic

Table 1

Specific rate constants $k(T; j)$ (cm^3 s^{-1}) for the F+H$_2$($v = 0, j = 0$–5) and F+D$_2$($v = 0, j = 0$–6) reactions as a function of temperature calculated on the SW PES. Numbers in parentheses represent powers of ten

F+H$_2$ reaction

T (K)	$j = 0$	$j = 1$	$j = 2$	$j = 3$
200	$1.17 \pm 0.03(-11)$	$1.84 \pm 0.05(-11)$	$2.28 \pm 0.05(-11)$	$2.70 \pm 0.06(-11)$
250	$2.09 \pm 0.05(-11)$	$3.03 \pm 0.06(-11)$	$3.66 \pm 0.06(-11)$	$4.24 \pm 0.07(-11)$
300	$3.14 \pm 0.05(-11)$	$4.34 \pm 0.07(-11)$	$5.13 \pm 0.07(-11)$	$5.84 \pm 0.07(-11)$
350	$4.27 \pm 0.06(-11)$	$5.69 \pm 0.07(-11)$	$6.63 \pm 0.07(-11)$	$7.44 \pm 0.08(-11)$
400	$5.44 \pm 0.06(-11)$	$7.05 \pm 0.08(-11)$	$8.12 \pm 0.08(-11)$	$9.01 \pm 0.08(-11)$
450	$6.61 \pm 0.07(-11)$	$8.40 \pm 0.08(-11)$	$9.58 \pm 0.08(-11)$	$1.05 \pm 0.01(-10)$
500	$7.78 \pm 0.07(-11)$	$9.71 \pm 0.08(-11)$	$1.10 \pm 0.01(-10)$	$1.20 \pm 0.01(-10)$

T (K)	$j = 4$	$j = 5$
200	$3.21 \pm 0.06(-11)$	$3.97 \pm 0.07(-11)$
250	$4.91 \pm 0.07(-11)$	$5.86 \pm 0.08(-11)$
300	$6.65 \pm 0.08(-11)$	$7.75 \pm 0.09(-11)$
350	$8.36 \pm 0.08(-11)$	$9.59 \pm 0.09(-11)$
400	$1.00 \pm 0.01(-10)$	$1.13 \pm 0.01(-10)$
450	$1.16 \pm 0.01(-10)$	$1.30 \pm 0.01(-10)$
500	$1.31 \pm 0.01(-10)$	$1.46 \pm 0.01(-10)$

F+D$_2$ reaction

T (K)	$j = 0$	$j = 1$	$j = 2$	$j = 3$
200	$0.47 \pm 0.02(-11)$	$0.67 \pm 0.02(-11)$	$0.99 \pm 0.03(-11)$	$1.13 \pm 0.03(-11)$
250	$0.93 \pm 0.03(-11)$	$1.25 \pm 0.03(-11)$	$1.74 \pm 0.04(-11)$	$1.96 \pm 0.04(-11)$
300	$1.49 \pm 0.03(-11)$	$1.95 \pm 0.04(-11)$	$2.59 \pm 0.04(-11)$	$2.88 \pm 0.04(-11)$
350	$2.13 \pm 0.04(-11)$	$2.70 \pm 0.04(-11)$	$3.50 \pm 0.05(-11)$	$3.86 \pm 0.05(-11)$
400	$2.82 \pm 0.04(-11)$	$3.50 \pm 0.04(-11)$	$4.42 \pm 0.05(-11)$	$4.86 \pm 0.05(-11)$
450	$3.53 \pm 0.04(-11)$	$4.31 \pm 0.05(-11)$	$5.35 \pm 0.05(-11)$	$5.85 \pm 0.05(-11)$
500	$4.26 \pm 0.05(-11)$	$5.13 \pm 0.05(-11)$	$6.27 \pm 0.05(-11)$	$6.82 \pm 0.05(-11)$

T (K)	$j = 4$	$j = 5$	$j = 6$
200	$1.26 \pm 0.03(-11)$	$1.44 \pm 0.03(-11)$	$1.65 \pm 0.04(-11)$
250	$2.14 \pm 0.04(-11)$	$2.39 \pm 0.04(-11)$	$2.70 \pm 0.05(-11)$
300	$3.12 \pm 0.05(-11)$	$3.44 \pm 0.05(-11)$	$3.82 \pm 0.05(-11)$
350	$4.13 \pm 0.05(-11)$	$4.52 \pm 0.05(-11)$	$4.96 \pm 0.06(-11)$
400	$5.16 \pm 0.06(-11)$	$5.59 \pm 0.06(-11)$	$6.08 \pm 0.06(-11)$
450	$6.19 \pm 0.06(-11)$	$6.66 \pm 0.06(-11)$	$7.18 \pm 0.06(-11)$
500	$7.19 \pm 0.06(-11)$	$7.69 \pm 0.06(-11)$	$8.25 \pm 0.06(-11)$

transition can be neglected. Interestingly, the QM thermal rate constants calculated with the mentioned coupled states excitation functions [24] are almost coincident with the QCT ones on 6SEC-PES [23] (see Table 2).

The QCT thermal rate constants for F+H$_2$ obtained in the present work are systematically larger than those reported for the 6SEC-PES; the difference decreases from a factor of 1.4 at 200 K to a factor 1.1 at 500 K. However, for the reaction of F with D$_2$, the classical $k(T)$ are practically identical on both the SW and 6SEC surfaces over the whole temperature region

Table 2
Thermal rate constants $k(T)$ (10^{-11} cm^3 s^{-1}) for the F+n-H$_2$ and F+n-D$_2$ reactions as a function of temperature calculated on the SW PES and taking into account the multisurface factor (see text)

F+H$_2$

T (K)	SW PES	Exp. WH[a]	Exp. SBA[b]	Exp. HBGM[c]	6SEC QCT[d]	6SEC QM[e]
200	0.86 ± 0.05	1.14			0.61	0.68
250	1.44 ± 0.06	1.76	1.83		1.13	1.19
300	2.07 ± 0.07	2.33	2.48	2.91	1.69	1.75
350	2.70 ± 0.07	2.89	3.14	3.92	2.32	2.37
400	3.32 ± 0.08			4.85	2.92	2.97
450	3.93 ± 0.08			5.73	3.50	
500	4.50 ± 0.08			6.54	4.06	

F+D$_2$

T (K)	SW PES	Exp. WH[a]	Exp. SBA[b]	Exp. HBGM[c]	6SEC QCT[d]	6SEC QM[e]
200	0.38 ± 0.03	0.57			0.36	0.43
250	0.72 ± 0.03	0.99	0.61		0.70	0.78
300	1.10 ± 0.04	1.41	0.95	1.39	1.08	1.15
350	1.51 ± 0.05	1.86	1.33	1.88	1.51	1.57
400	1.91 ± 0.05			2.34	1.92	1.96
450	2.30 ± 0.05			2.76	2.33	
500	2.68 ± 0.05			3.16	2.71	

[a] Ref. [30]. [b] Ref. [32]. [c] Ref. [31]. [d] Ref. [23]. [e] Ref. [24].

considered. This interesting difference in the reactivity predicted on the two PES can be traced back to the distinct influence of rotation at threshold (see Fig. 2) and to the different distribution of rotational states corresponding to each of the isotopic variants. Over the temperature range considered, the $j = 1$ state is preponderant in n-H$_2$ and its excitation function has a lower threshold on the SW surface. At 300 K, for instance, the relative populations of the three first rotational levels $j = 0, 1, 2$ are 0.13, 0.66, 0.12, respectively. Inspection of Fig. 2 shows that, for the F+H$_2$ reaction, this distribution of rotational levels will lead to a higher thermal rate constant on the SW surface. In normal deuterium, the relative populations of the lowest states, $j = 0, 1, 2, 3$ at a temperature of 300 K are 0.18, 0.20, 0.38 and 0.11 respectively. The most populated level is $j = 2$, whose excitation function has a somewhat lower threshold on the SW than on the 6SEC surface; however, the slightly larger reaction cross-sections found for $j = 2, 3$ on the SW-PES as compared to the 6SEC one are compensated by the somewhat smaller values obtained for $j = 0, 1$ (see

Fig. 2b).

The QCT rate constants calculated on the SW-PES are in reasonable agreement with the measurements, but except for the experiment of Stevens et al. [32] for F+D$_2$, the theoretical values are somewhat lower than the experimental data. The largest discrepancies are found for the F+H$_2$ isotopic variant where over the higher temperature range studied (350–500 K) the experimental measurements of Heidner et al. [31] are about a factor of 1.4 larger than those from the present calculations. It is interesting to note that in the case of F+H$_2$, the agreement between the experiment and the $k(T)$ obtained on the SW-PES is better than with the $k(T)$ calculated on the 6SEC-PES [23,24]. This difference in the rate constants on the two PESs can be traced back to the larger cross section values obtained for the SW-PES at low collision energies.

The fact that the QM cross sections obtained on the SW-PES [26] at low energies are higher than the classical ones, mainly for $j = 0$, leads to larger QM rate constants at low temperature. In the case of F+H$_2$ these approximate QM $k(T)$ are even larger than the
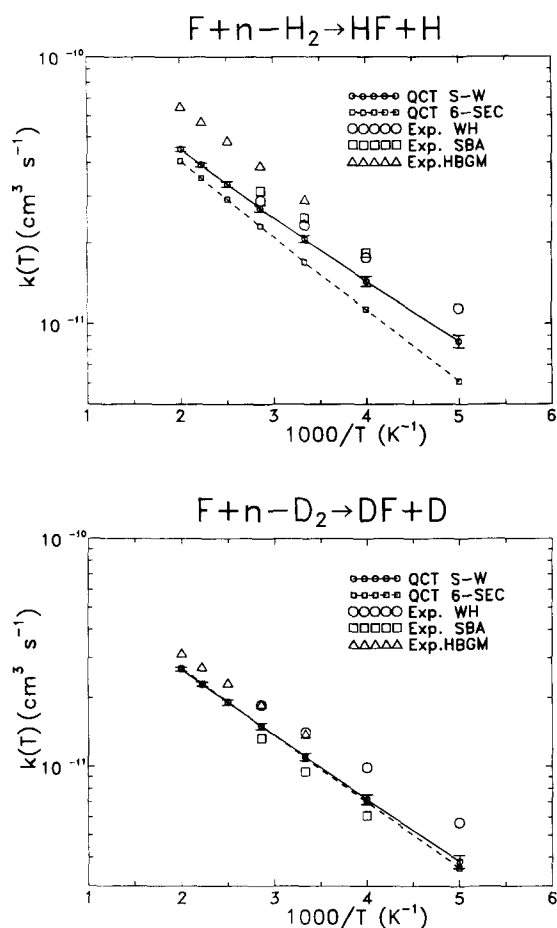
$$F+n-H_2 \rightarrow HF+H$$

$$F+n-D_2 \rightarrow DF+D$$

$$F+n-H_2/F+n-D_2$$

Fig. 4. Ratio of the rate constants for the $F+n$-H_2 and $F+n$-D_2 reactions as a function of the temperature (kinetic isotope effect). The squares are experimental data from Ref. [33]. The small squares connected by a solid line: QCT calculations on the 6SEC-PES; circles connected by a solid line: present calculations on the SW-PES.

Fig. 3. Comparison of thermal rate constants from experiment and theory for the reaction of fluorine atoms with hydrogen (deuterium) molecules (see Table 1). Upper panel: $F+H_2$; lower panel: $F+D_2$. The small circles with error bars connected by a solid line are the results of the present calculations. The small squares connected by a dashed line are the QCT calculations of Rosenman and Persky [23] on the 6SEC-PES. The large circles correspond to the experimental data of Wurzberg and Houston [30], the large squares to the points of Stevens et al. [32] and the triangles are the measurements of Heidner et al. [31].

experimental ones for temperatures lower than 250 K. As mentioned above, the inclusion of the spin–orbit coupling in the ab initio calculations of the PES is expected to increase the barrier height, and this should lead to a better agreement between QM calculations and experimental results, whereas the QCT calculations will probably underestimate the rate constants, especially at low temperatures. At $T > 300$ K, the QM $k(T)$ become smaller than the measurements, and sim-
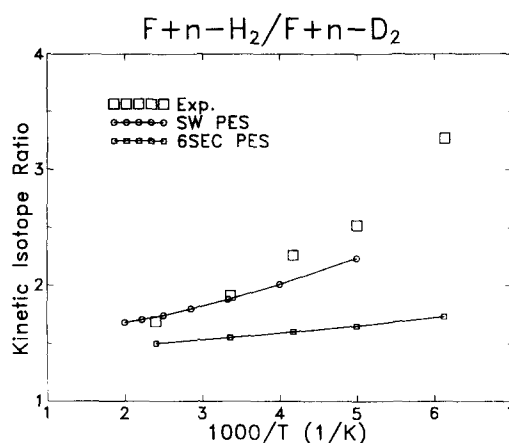
ilar to the QCT ones. A possible explanation for this high temperature discrepancy between experiment and both theoretical approaches would be the contribution of non–adiabatic channels to the reaction, which are explicitly excluded from the present theoretical results through the use of the 'multisurface correction factor'. The discrepancy between QCT and QM results at low T is most probably due to tunneling [25].

Fig. 4 displays the kinetic isotopic ratio of the rate constants, k_{F+H_2}/k_{F+D_2} as a function of the temperature. The present results are in much better agreement with the experimental results of the direct determination of the kinetic isotope effect of refs. [33,34] than those obtained on the 6SEC-PES [23]. The QCT results on the SW-PES predict a stronger isotope effect than the one obtained on the 6SEC-PES, which, however, at temperatures below 250 K is still smaller than the one found experimentally.

Besides the experimental thermal rate constants just commented on, the only estimate of the reactive 'size' for this system is provided by the absolute value of the reaction cross section determined by Faubel et al. [5] in a crossed molecular beams experiment for $F+D_2$. The corresponding cross section value calculated from QCT on the SW-PES was found to be within the experimental uncertainty [21]

4. Conclusions

The reasonably good agreement between QCT thermal rate constants calculated on the present ab initio PES and the measured values indicates that this surface is more accurate than any previous one, not only in its shape, as already shown in previous calculations of differential cross sections and the electron photodetachment spectrum of FH_2^-, but also in the height of its barrier. However, the comparison with quantum mechanical calculations indicates that tunneling effects make the translational thresholds lower than the classical ones and the net effect is to increase the rate constants at low temperatures, in particular for F + H_2, above the experimental values. An increase in the barrier height due to spin-orbit effects in the entrance channel will have the opposite effect. Although the present calculations corroborate the global accuracy of the PES, a definite conclusion about the finest details of the PES cannot be drawn from the present results.

Acknowledgement

References

|1| D.M. Neumark, A.M. Wodtke, G.N. Robinson, C.C. Hayden and Y.T. Lee, J. Chem. Phys. 82 (1985) 3045

|2| D.M. Neumark, A.M. Wodtke, G.N. Robinson, C.C. Hayden, R. Shobatake, R.K. Sparks, T.P. Schafer and Y.T. Lee, J. Chem. Phys. 82 (1985) 3067.

|3| D.E. Manolopoulos, K. Stark, H.-J. Werner, D.W. Arnold, S.E. Bradforth and D.M. Neumark, Science 262 (1993) 1852.

|4| S.E. Bradforth, D.W. Arnold, D.M. Neumark and D.E. Manolopoulos, J. Chem. Phys. 99 (1993) 6345.

|5| M. Faubel, L. Rusin, S. Schlemmer, F. Sondermann, U. Tappe and J.P. Toennies, J. Chem. Phys. 101 (1994) 2106.

|6| M. Faubel, B. Martinez-Haya, L.Y. Rusin, U. Tappe and J.P. Toennies, Chem. Phys. Letters 232 (1995) 197.

[7] M. Faubel, B. Martinez-Haya, L.Y. Rusin, U. Tappe and J.P. Toennies, Z. Physik. Chem. 188 (1995) 197.

[8] F.B. Brown, R. Steckler, D.W. Schwenke, D.G. Truhlar and B.C. Garrett, J. Chem. Phys. 82 (1985) 188;
R. Steckler, D.G. Truhlar and B.C. Garrett, J. Chem.Phys. 82 (1985) 5499.

[9] T. Takayanagi and S. Sato, Chem. Phys. Letters 144 (1988) 191.

[10] G.C. Lynch, R. Steckler, D.W. Schwenke, A.J.C. Varandas and D.G. Truhlar, J. Chem. Phys. 94 (1991) 7150.

[11] S.L. Mielke, G.C. Lynch, D.G. Truhlar and D.W. Schwenke, Chem. Phys. Letters 213 (1993) 11; 217 (1994) 173 (E).

[12] P.J. Knowles, K. Stark and H.-J. Werner, Chem. Phys. Letters 185 (1991) 555.

[13] K. Stark and H.-J. Werner, J. Chem. Phys. (1996), in press.

[14] J.Z.H. Zhang, W.H. Miller, A. Weaver and D. Neumark, Chem. Phys. Letters 182 (1991) 283.

[15] J.M. Launay and M. Le Dourneuf, Chem. Phys. Letters 169 (1990) 473.

[16] J.M. Launay, Theoret. Chim. Acta 79 (1991) 183.

[17] F.J. Aoiz, V.J. Herrero, M.M. Nogueira and V. Sáez Rábanos, Chem. Phys. Letters 204 (1993) 359.

[18] F.J. Aoiz, L. Bañares, V.J. Herrero and V. Sáez Rábanos, Chem. Phys. Letters 218 (1994) 422.

[19] F.J. Aoiz, L. Bañares, V.J. Herrero and V. Sáez Rábanos, Chem. Phys. 187 (1994) 227.

[20] F.J. Aoiz, L. Bañares, V.J. Herrero, V. Sáez Rábanos, K. Stark and H.-J. Werner, Chem. Phys. Letters 223 (1994) 215.

[21] F.J. Aoiz, L. Bañares, V.J. Herrero,V. Sáez Rábanos, K. Stark and H.-J. Werner, J. Phys. Chem. 98 (1994) 10665.

[22] F.J. Aoiz, L. Bañares, V.J. Herrero, V. Sáez Rábanos, K. Stark and H.-J. Werner, J. Chem. Phys. 102 (1995) 9248.

[23] E. Rosenman and A. Persky, Chem. Phys. 195 (1995) 291.

[24] E. Rosenman, S. Hochman-Kowal, A. Persky and M. Baer, J. Phys. Chem. 99 (1995) 16523.

[25] J.F. Castillo, D.E. Manolopoulos, K. Stark and H.-J Werner, J. Chem. Phys. (1996), in press.

[26] M. Baer, H. Szichman, E. Rosenman, S. Hochman-Kowal and A. Persky, in: Gas phase chemical reaction systems: experiments and models, eds. J. Wolfrum, H-R. Volpp, R. Rannacher and J. Warnatz, Springer series in chemical physics (Springer, Berlin, 1996), in press.

[27] F.J. Aoiz, V.J. Herrero and V. Sáez Rábanos, J. Chem. Phys. 97 (1992) 7423.

[28] F.J. Aoiz, L. Bañares, T. Diez-Rojo, V.J. Herrero and V. Sáez Rábanos, J. Phys. Chem. (1996), in press.

[29] V.M. Azriel, G.D. Billing, L. Yu. Rusin and M.B. Sevryuk Chem. Phys. 195 (1995) 243.

[30] E. Wurzberg and P.L. Houston, J. Chem. Phys. 72 (1980) 4811.

[31] R.F. Heidner, J.F. Bott, C.E. Gardner and J.E. Melzer, J. Chem. Phys. 72 (1980) 4815.

[32] P.S. Stevens, W.H. Brune and J.G. Anderson, J. Phys. Chem. 93 (1989) 4068.

[33] A. Persky, J. Chem. Phys. 59 (1973) 3612.

[34] E.R. Grant and J.W. Root, J. Chem. Phys. 63 (1975) 2970.